Supporting Information

Enhanced capture ability of sludge-derived mesoporous biochar with template-like method

Wang Xin[a,b,c], Yonghui Song*[b,c], Yahan Wu[d]

a. Inner Mongolia Key Laboratory of Environmental Chemistry, College of Chemistry and Environmental Science, Inner Mongolia Normal University, Huhhot, 010022, PR China.

b. State Key Laboratory of Environmental Criteria and Risk Assessment, Chinese Research Academy of Environmental Sciences, Dayangfang 8, Anwai Beiyuan, Beijing 100012, PR China.

c. Department of Urban Water Environmental Research, Chinese Research Academy of Environmental Sciences, Dayangfang 8, Anwai Beiyuan, Beijing 100012, PR China.

d. State Key Laboratory of Alternate Electrical Power System with Renewable Energy Sources, North China Electric Power University, Beijing 102206, P. R. China.

**Corresponding author. E-mail: songyh@craes.org.cn; Fax: +86 10 84915194; Tel: +86 10 84915308*

Pages 15

Figures 5

Tables 10

Material characterization

For N_2-adsorption experiment, all samples were degassed overnight starting at room temperature, increasing to 120 °C at a increment step of 15°C every 15 min, and staying there for more than 10h, and the specific surface area (SSA) (S_{BET}), the micropore SSA (S_{micro}), total pore volume (V_t) and micropore volume (V_{micro}) were calculated. The SSA was calculated by the Brunauer-Emmett-Teller (BET) method and the pore size distributions were measured by Barrett-Joyner-Halenda (BJH) analysis from the desorption branch of the isotherms. The total pore volumes were estimated on the basis of the N_2 volume adsorbed at a relative saturation pressure P/P_0=0.99, which actually corresponded to the total amount adsorbed. The average pore diameter was determined from the SSA and total pore volume. The micropore volume was calculated from the t-plot method. XRF conditions were the following: voltage 9.0 kV, current 280 A, count time 100 s, warm-up 3 min. Instrument reference temperature was 293 K and background conditions: lower ROI 3200, upper ROI 5750 keV.

Table S1. The proximate analysis and basic element distribution of the used sludge.

Sample	Proximate analysis (wt %)				Elemental analysis (wt %)				
	M(%)	A(%)	V(%)	F(%)	H	S	N	C	O*
SS	6.83	37.96	53.66	1.55	6.35	1.79	4.31	33.72	15.87
SS-AC	1.37	78.88	2.73	17.02	0.51	0.67	2.82	15.43	1.69
SS-MBC	0.56	88.1	1.99	9.35	0.57	0.64	0.71	8.01	1.97

M: moisture content, A: ash content, V: volatile content, F: fixed carbon content, O*: difference method.

Table S2. The main component in the ash of the used sludge.

Main component	The content (wt %)
SiO_2	10.47
P_2O_5	7.28
Al_2O_3	5.96
CaO	4.06
Fe_2O_3	2.69
MgO	1.81
K_2O	1.51
S	1.14
Na_2O	0.374
TiO_2	0.294
ZnO	0.124
Cl	0.109

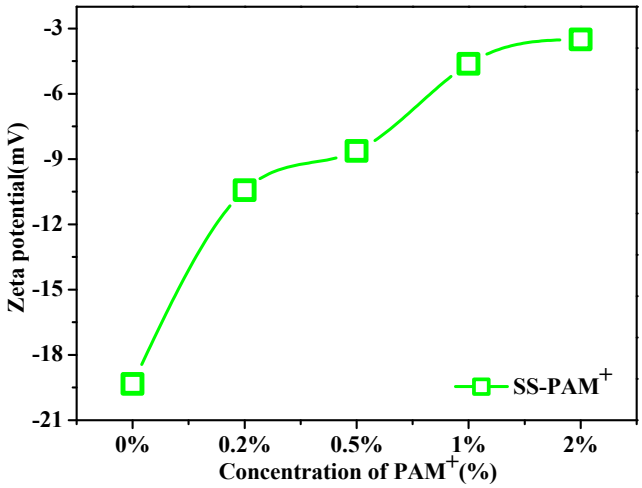

Figure S1. The Zeta-potential of flocculating constituent (SS-PAM$^+$) under different concentrations of PAM$^+$.

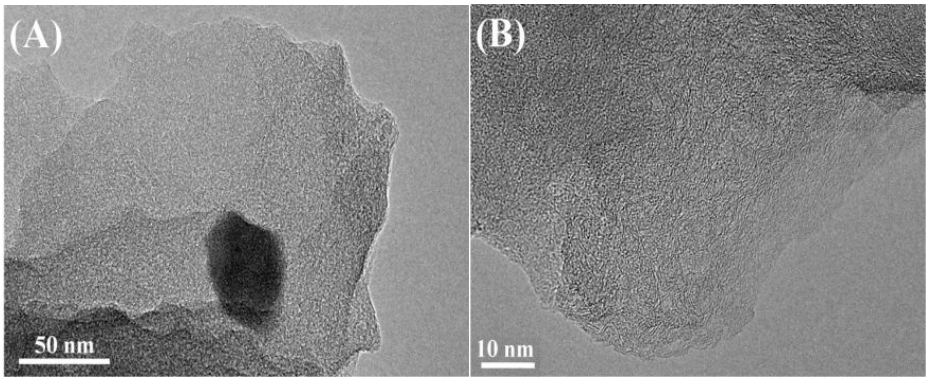

Figure S2. TEM images of the optimized SS-MBC sample with different magnification.

Table S3. Structural parameters of SS-AC, SS-MBC and AC.

Sample	S_{BET} (m^2/g)	S_{micro} (m^2/g)	S_{micro}/S_{BET}(%)	V_{total} (cm^3/g)	V_{micro} (cm^3/g)	V_{meso} (cm^3/g)	D_p (nm)
SS-AC	58.45	8.27	14.15	0.075	0.003	0.072	3.95
SS-MBC	116.42	52.76	45.32	0.143	0.024	0.119	4.9
AC	569.24	174.94	30.73	0.428	0.078	0.35	3.38

BET SSA (S_{BET}), micropore SSA (S_{micro}), micropore volume (V_{micro}), total pore volume (V_{total}), mesoporous volume (V_{meso}) and average pore diameter (D_p).

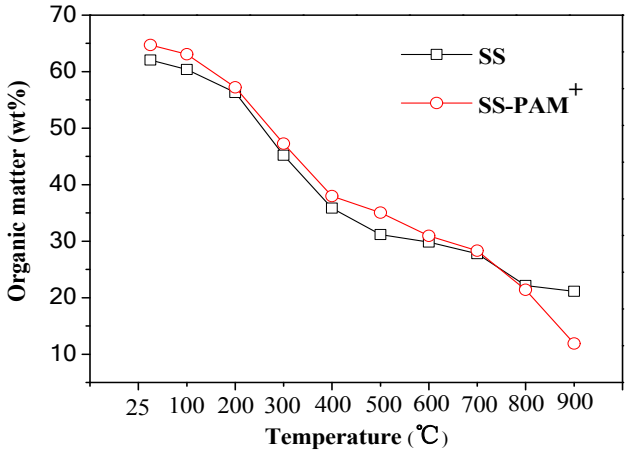

Figure S3. Changes of the organic matter during the pyrolysis process for SS and SS-PAM^{+}.

Table S4. Concentrations of the surface functional groups of the samples.

Samples	Carboxylic (mmol/g)	Lactonic (mmol/g)	Phenolic (mmol/g)	Total acidic (mmol/g)	Basic (mmol/g)
SS-MBC	0.546	0.337	1.564	2.447	0.315
SS-AC	0.283	0.108	1.288	1.679	0.295
AC	0.176	0.144	0.867	1.187	0.267

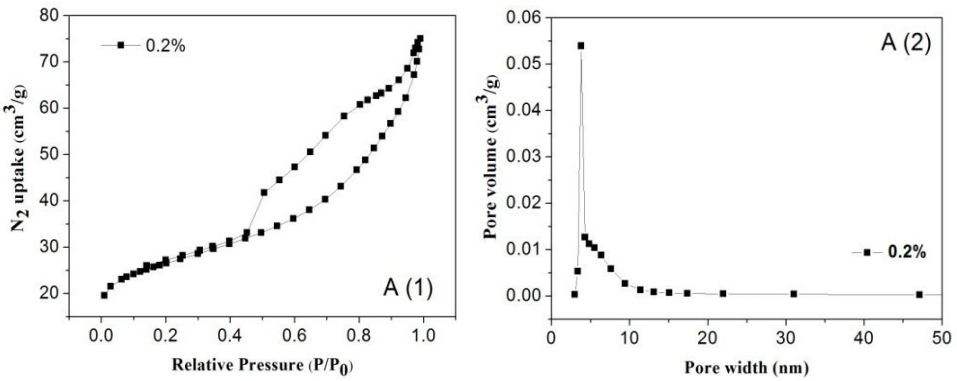

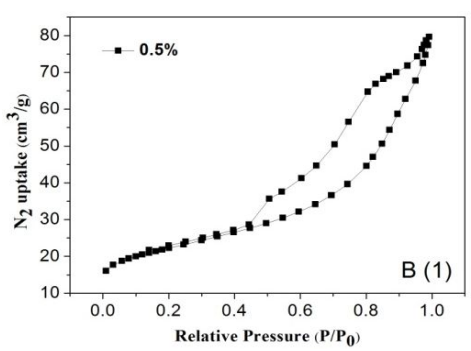
0.5%
B (1)
N2 uptake (cm3/g)
Relative Pressure (P/P0)

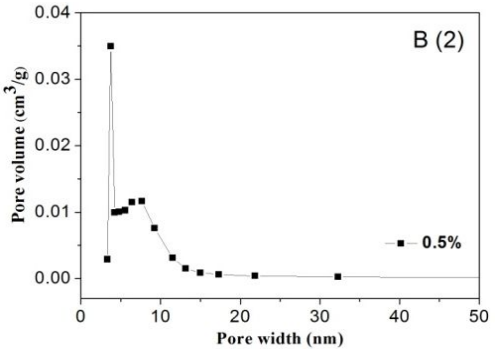
B (2)
0.5%
Pore volume (cm3/g)
Pore width (nm)

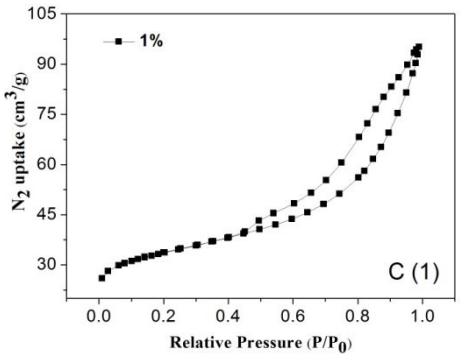
1%
C (1)
N2 uptake (cm3/g)
Relative Pressure (P/P0)

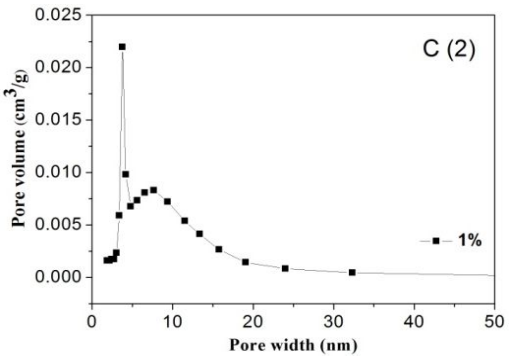
C (2)
1%
Pore volume (cm3/g)
Pore width (nm)

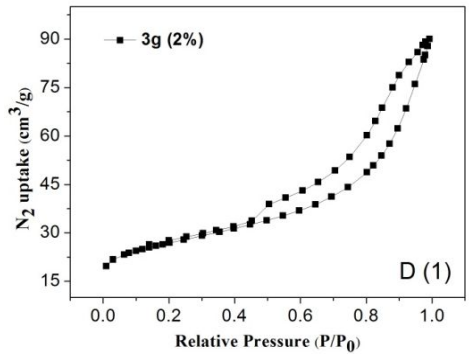
3g (2%)
D (1)
N2 uptake (cm3/g)
Relative Pressure (P/P0)

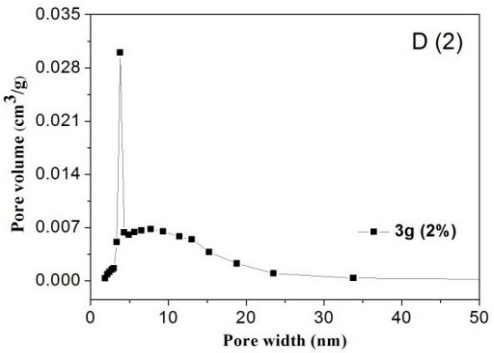
D (2)
3g (2%)
Pore volume (cm3/g)
Pore width (nm)

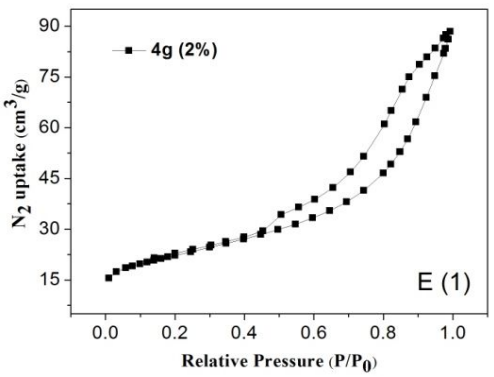
4g (2%)
E (1)
N2 uptake (cm3/g)
Relative Pressure (P/P0)

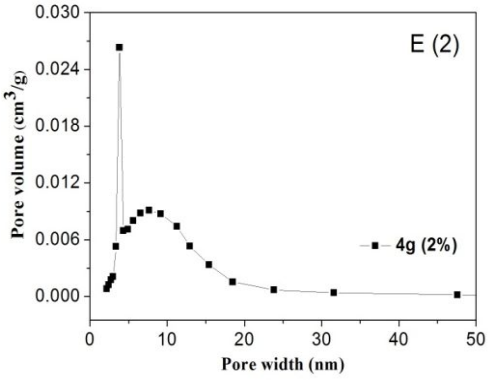
E (2)
4g (2%)
Pore volume (cm3/g)
Pore width (nm)

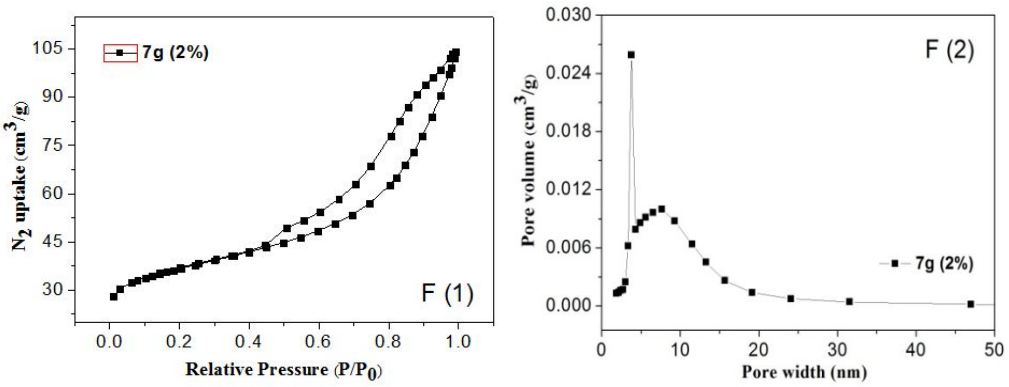

Figure S4. Carbonization and drying at 900℃ and 60℃, respectively: A(1)A(2), B(1)B(2), C(1)C(2), D(1)D(2), E(1)E(2), F(1)F(2) presented N_2 adsorption-desorption isotherm and corresponding BJH pore size distribution of SS-MBC-0.2-5, SS-MBC-0.5-5, SS-MBC-1-5, SS-MBC-2-3, SS-MBC-2-4, SS-MBC-2-7, respectively.

Table S5. Structural information of biochars from different synthesis parameters.

Samples	[a]S_{BET} (m^2/g)	[b]S_{mic} (m^2/g)	[c]V_t (cm^3/g)	[d]V_{mic} (cm^3/g)	[e]D_m (nm)
SS-AC	58.45	8.27	0.075	0.003	3.95
SS-MBC-0.2-5	77.66	26.83	0.104	0.012	4.53
SS-MBC-0.5-5	91.82	39.49	0.112	0.018	4.63
SS-MBC-1-5	115.41	59.58	0.135	0.028	4.68
SS-MBC-2-5	116.42	52.76	0.143	0.024	4.9
SS-MBC-2-3	78.13	21.66	0.127	0.0097	5.55
SS-MBC-2-4	93.16	38.43	0.129	0.018	6.48

SS-MBC-2-7	126.26	62.19	0.15	0.0287	4.76

[a]BET SSA. [b]Micropore area. [c]Total pore volume. [d]Micropore pore volume. [e]Average pore diameter.

Adsorption experiments

1.1 Effect of different preparation factors to removal efficiency

In this section, we prepared samples under different preparation conditions, the concrete experimental plans have been shown in Table S6. 20 mg prepared sample was added to 50 mL MB solution in conical flask and agitated in the shaker at 25 ± 1℃ and a rate of 150 rpm. The initial pH of the MB solution was adjusted to 7.0 ± 0.1 by 0.1 M NaOH and HCl solutions. After 24 h, aqueous sample was taken for analysis of MB equilibrium concentration.

Table S6. Effect of different preparation factors to removal efficiency.

Teams	Investigation factors	PAM^+ concentration (%)	Additive sludge (g)	Drying type	Carbonization temperature (℃)
1	PAM^+ concentration	0.2	5	105℃	900℃
2		0.5	5	105℃	900℃
3		1	5	105℃	900℃
4		2	5	105℃	900℃
5	Additive sludge	2	3	105℃	900℃
6		2	4	105℃	900℃
7		2	5	105℃	900℃
8		2	6	105℃	900℃
9		2	7	105℃	900℃

10		2	8	105℃	900℃
11		2	9	105℃	900℃
12	Drying method	2	5	180℃	900℃
13		2	5	140℃	900℃
14		2	5	105℃	900℃
15		2	5	60℃	900℃
16		2	5	6000r/min	900℃
17	Carbonization temperature	2	5	60℃	500℃
18		2	5	60℃	600℃
19		2	5	60℃	700℃
20		2	5	60℃	800℃
21		2	5	60℃	900℃

1.2 Effect of aqueous pH

The aqueous effect of pH on MB sorption (200 mg/L) onto SS-MBC and SS-AC samples was examined at different pH values (pH 2, 3, 4, 5, 6, 7, 8, 9 and 10). The pH was adjusted with NaOH and HCl solutions.

1.3 Sorption isotherms

Sorption isotherms of MB were determined by adding 0.02 g SS-MBC-2-5, SS-MBC-1-5, SS-MBC-0.5-5, SS-MBC-0.2-5 and SS-AC with 50 mL MB solution of different initial concentrations ranging from 100 to 200 mg/L in the conical flasks. The initial pH of the suspension was adjusted to 10.0 ± 0.1 by 0.1 M NaOH and HCl solutions. The conical flasks were shaken in the dark at 25 ±1℃ for 24 h. All the experiments were conducted in triplicate, and the

results were calculated as the mean values.

The commonly isotherm models, namely Langmuir and Freundlich were used to describe the adsorption of methylene blue onto sludge-adsorbents. The Langmuir isotherm indicates monolayer adsorption onto a completely homogeneous surface, and is given as

$$q_e = \frac{Q \cdot b \cdot C_e}{1 + b \cdot C_e} \quad \text{(S1)}$$

where Q (mg/g) is the maximum uptake per unit mass of adsorbent to form a complete monolayer on the surface of adsorbent, and b (L/mg) is a constant related to the affinity of the binding sites. The essential feature of a Langmuir isotherm can be expressed in accordance with a dimensionless constant separation factor or equilibrium parameter, R_L, which is defined as

$$R_L = \frac{1}{1 + bC_0} \quad \text{(S2)}$$

where C_0 (mg/L) is the initial dye concentration and b (L/mg) is the Langmuir isotherm constant. The $R_L$valuesindicate the type of the isotherm to be unfavorable (R_L> 1), linear (R_L= 1), favorable (0 < R_L< 1), irreversible (R_L= 0).

The empirical Freundlich isotherm based on sorption on a heterogeneous surface is given by

$$q_e = K_F \cdot C_e^{\frac{1}{n}} \quad \text{(S3)}$$

where K_F and 1/n are the Freundlich constants which are indicators of the maximum adsorption capacity and intensity, respectively.

1.4 Sorption kinetics

For MB kinetic experiment, briefly, 250 ml MB solution (150 mg/L) and 0.25 g sorbent samples (SS-MBC, SS-AC, AC) were placed in a 500 mL conical flask. The initial pH of the solution was

adjusted to 10.0 ± 0.1 with 0.1 M NaOH and HCl solution. All the conical flasks were agitated in shaker at 25 ± 1℃ and a rate of 150 rpm. One milliliter of sample was taken at 10, 20, 30, 60, 90, 120, 150, 180, 240, 300, 360, 420 and 480 min for analysis of MB concentration. All the experiments were conducted in triplicate, and the results were calculated as the mean values. The kinetics studies were performed by measuring the residual concentration of MB at preset time intervals. The kinetics data was usually evaluated by using two kinetics models, namely pseudo-first-order and Ho's pseudo-second-order models. Pseudo-first-order model is given by

$$q_t = q_e(1 - e^{-k_1 t}) \quad \text{(S4)}$$

where q_t (mg/g) is the amounts of MB adsorbed at time t (min), and k_1(min^{-1}) is the rate constant of first-order adsorption. The applicability of pseudo-first-order model indicates that the external diffusion is a significant step. Ho's pseudo-second-order equation based on chemical related adsorption is expressed as

$$q_t = \frac{k_2 q_e^{\,2} t}{1 + k_2 q_e t} \quad \text{(S5)}$$

where k_2 (g/mg·min) is the rate constant of pseudo-second-order adsorption.

1.5 Heavy metal leaching test

Experiments were conducted to study the effect of pH of the solution (pH=3.5) on heavy metals leaching from biochar samples (SS-AC, SS-MBC). The solid sample (5 g) was mixed with 50 mL of distilled water and the pH of the solution was adjusted to the desired value by addition of 0.1 N HCl/NaOH solutions. The solution was kept for 24 h and was filtered using 0.45 μm nylon filter. The resultant filtrate was analyzed for heavy metals using atomic absorption spectrophotometer for the six heavy metals (Cr, Cu, Ni, Zn, Pb, and Cd).

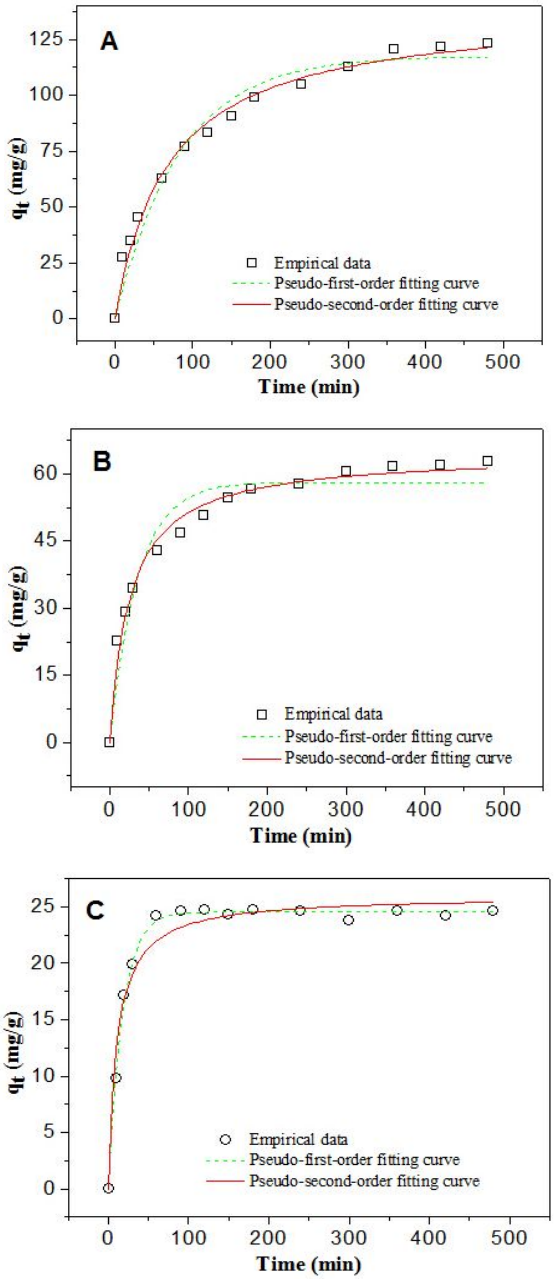

Figure S5. Comparison of the pseudo-first-order and pseudo-second-order models for MB on (A) SS-MBC, (B) SS-AC, (C) AC.

Table S7. Isotherm constants of MB removal onto SS-MBCs.

Adsorbent	Q_{mea}	Langmuir model				Freundlich model		
		Q_{cal}(mg/g)	b(L/mg)	R_L	R^2	K_F(mg/g)(L/mg)$^{1/n}$	n	R^2
SS-MBC-2-5	380.67	386.19	0.888	0.007	0.984	267.85	10.75	0.886
SS-MBC-1-5	350.06	372.65	0.249	0.023	0.987	199.62	7.21	0.901
SS-MBC-0.5-5	314.72	345.68	0.143	0.039	0.983	159.79	6.26	0.897
SS-MBC-0.2-5	278.12	314.76	0.085	0.065	0.99	117.31	5.72	0.952
SS-MBC-0-5	238.09	266.78	0.074	0.074	0.988	105.1	5.17	0.934

Q_{mea}: experimental maximum uptake; Q_{cal}: calculated maximum uptake.

Table S8. Kinetics constants of MB removal onto adsorbents.

Adsorbent	q_{mea} (mg/g)	Pseudo-first order model			Pseudo-second order model		
		q_{cal} (mg/g)	k_1 (min^{-1})	R^2	q_{cal} (mg/g)	k_2(g/mg·min) $\times 10^{-4}$	R^2
SS-MBC	123.39	117.58	0.056	0.945	138.84	8.041	0.988
SS-AC	62.69	58.12	0.028	0.938	64.51	6.017	0.987
AC	24.62	24.55	0.012	0.997	25.99	3.254	0.959

q_{mea}: experimental maximum uptake; q_{cal}: calculated maximum uptake.

Table S9. Concentration of different metals (mg/L) in pristine sewage or leachate.

Samples	Cu	Cr	Ni	Pb	Zn	Cd
SS	144	89.2	28.7	50.3	742	2.81
SS-AC	<0.01	<0.03	0.041	<0.01	3.30	<0.01
SS-MBC	<0.01	<0.03	0.057	<0.01	0.29	<0.01
Permissible limits	50	10	10	3	50	0.3

Table S10. Comparison of the adsorption capacities of MB onto different sludge-based adsorbents.

Precusors	q_{max} (mg/g)	Ref.
NaOH + sludge	66.23	[1]
Sludge and tea waste	19.38	[2]
KOH and sludge	87.50	[3]
Sludge	29.85	[4]
Sludge	11.78	[5]
Sludge and $FeCl_3 \cdot 6H_2O$	50.00	[6]
Sludge and pine sawdust	16.75	[7]
Sludge	285.70	[8]
PAM^+ + sludge	123.39	This work

References

[1] K. Gobi, M.D. Mashitah, V.M. Vadivelu, Adsorptive removal of Methylene Blue using novel adsorbent from palm oil mill effluent waste activated sludge: Equilibrium, thermodynamics and

kinetic studies, Chemical Engineering Journal 171 (2011) 1246-1252.

[2] S. Fan, J. Tang, Y. Wang, H. Li, H. Zhang, J. Tang, Z. Wang, X. Li, Biochar prepared from co-pyrolysis of municipal sewage sludge and tea waste for the adsorption of methylene blue from aqueous solutions: Kinetics, isotherm, thermodynamic and mechanism, Journal of Molecular Liquids 220 (2016) 432-441.

[3] W.H. Shen, Q.J. Guo, H. Wang, X.P. Yang, Y.H. Liu, Y.L. Zhang, Product composition of pyrolyzed sewage sludge and adsorption of methylene blue by porous material derived from it, Environmental Engineering Science 25 (2008) 99-105.

[4] S. Fan, Y. Wang, Z. Wang, J. Tang, J. Tang, X. Li, Removal of methylene blue from aqueous solution by sewage sludge-derived biochar: Adsorption kinetics, equilibrium, thermodynamics and mechanism, Journal of Environmental Chemical Engineering 5 (2017) 601-611.

[5] H.D. Utomo, X.C. Ong, S.M.S. Lim, G.C.B. Ong, P. Li, Thermally processed sewage sludge for methylene blue uptake, International Biodeterioration & Biodegradation 85 (2013) 460-465.

[6] Nhamo, Chaukura, C. Edna, Murimba, Willis, Gwenzi, Sorptive removal of methylene blue from simulated wastewater using biochars derived from pulp and paper sludge, Environmental Technology & Innovation 8 (2017) 275-287.

[7] G. Cheng, L. Sun, L. Jiao, L. Peng, Z. Lei, Y. Wang, J. Lin, Adsorption of methylene blue by residue biochar from copyrolysis of dewatered sewage sludge and pine sawdust, Desalination & Water Treatment 51 (2013) 7081-7087.

[8] C.C. Liu, Y.S. Li, Y.M. Chen, H.H. Li, M.K. Wang, Removal of methylene blue from aqueous solution using wine-processing waste sludge, Water Science & Technology A Journal of the International Association on Water Pollution Research 65 (2012) 2191-2208.